Electric field modulation technique for high-voltage AlGaN/GaN Schottky barrier diodes*

Tang Cen(汤 岑)[a], Xie Gang(谢 刚)[a]†, Zhang Li(张 丽)[b], Guo Qing(郭 清)[a], Wang Tao(汪 涛)[a], and Sheng Kuang(盛 况)[a]

[a] College of Electrical Engineering, Zhejiang University, Hangzhou 310007, China
[b] Division of Energy, High Technology Research and Development Center, the Ministry of Science and Technology, Beijing 100044, China

(Received 27 February 2013; revised manuscript received 9 April 2013)

A novel structure of AlGaN/GaN Schottky barrier diode (SBD) featuring electric field optimization techniques of anode-connected-field-plate (AFP) and magnesium-doped p-type buried layer under the two-dimensional electron gas (2DEG) channel is proposed. In comparison with conventional AlGaN/GaN SBDs, the magnesium-doped p-type buried layer in the proposed structure can provide holes that can help to deplete the surface 2DEG. As a result, surface field strength around the electrode edges is significantly suppressed and the electric field along the channel is distributed more evenly. Through 2D numerical analysis, the AFP parameters (field plate length, L_{AFP}, and field plate height, T_{AFP}) and p-type buried layer parameters (p-type layer concentration, N_P, and p-type layer thickness, T_P) are optimized to achieve a three-equal-peak surface channel field distribution under exact charge balance conditions. A novel structure with a total drift region length of 10.5 μm and a magnesium-doped p-type concentration of 1×10^{17} cm^{-3} achieves a high breakdown voltage (V_B) of 1.8 kV, showing 5 times improvement compared with the conventional SBD with the same device dimension.

Keywords: gallium nitride, high voltage SBD, field plate, magnesium buried layer

PACS: 61.72.uj, 71.20.N, 51.50.+v **DOI:** 10.1088/1674-1056/22/10/106107

1. Introduction

Owing to the outstanding properties of high sheet carrier density, high mobility in the two-dimensional electron gas (2DEG) channel and high critical electric field, the GaN-based heterostructure Schottky barrier diode (SBD) shows superior performance for high power switching applications.[1] Newly developed high-quality silicon epitaxial substrate with cost effectiveness stimulates wide use of the GaN device in the power field.[2,3] Meanwhile, in the desire of reducing power losses, several electric field modulation techniques are utilized to increase the breakdown voltage (V_B) and suppress the leakage current of the AlGaN device. Field plate (FP) technologies are commonly used to extend the depletion region by the FP geometry.[4,5] Floating rings (FR) technologies are introduced considering the charge-coupling effect.[6] Partial doping methods including fluorine, silicon, and carbon are also reported to be effective in modulating the electric fields.[7–10] However, the maximum V_B is far from theoretical values for a given drift region length, obtained using these methods, due to the premature breakdown which still happens along the surface of the devices.[11,12]

In this paper, we study the effect of the electric field modulation techniques on the breakdown voltage. Silvaco 2D numerical tool is used to analyze the detailed electrical characteristics of the device. In particular, we evaluate the breakdown performance, as well as the electric field profiles of the AlGaN/GaN SBD using an anode-connected-field-plate and a magnesium-doped p-type buried layer, namely AFP-RESURF-SBD. The AFP height (T_{AFP}), AFP length (L_{AFP}), p-type buried layer thickness (T_P), and doping concentration (N_P) are all investigated.

2. Device structure and simulation model

Devices of conventional AlGaN/GaN Schottky barrier diode (Con. SBD), anode-connected-field-plate AlGaN/GaN Schottky barrier diode (AFP-SBD) and AFP-RESURF-SBD are shown in Fig. 1. The magnesium-doped p-type buried layer is located 0.1 μm underneath the 2DEG channel. All the devices of Con. SBD, AFP-SBD, and AFP-RESURF-SBD have the same device physical dimensions as shown in Figs. 1(a)–1(c). The epitaxial layer structure consists of a GaN buffer layer (2 μm)/unintentionally-doped (UID) AlGaN barrier layer (25 nm). Al mole fraction in the AlGaN layer is 0.15. The thickness of the SiN passivation layer is set to be 500 nm considering the empirical experimental parameters. A sheet carrier density of 7.5×10^{12} cm^{-2} caused by the polarization in wurzite materials is modeled by the spontaneous polarization, P_{sp}, and piezoelectric polarization, P_{pi} to determine

*Project supported by the Science Foundation of the Ministry of Education of China (Grant No. 20100101110056) and the Natural Science Foundation of Zhejiang Province of China for Distinguished Young Scholars (Grant No. R1100468).

†Corresponding author. E-mail: xielyz@zju.edu.cn

© 2013 Chinese Physical Society and IOP Publishing Ltd

the 2DEG sheet carrier concentration. In order to simulate the avalanche breakdown of the device, the Selberherr impact ionization-generation model with user-definable impact ionization parameters is used.[13] Other device parameter values employed for simulation are listed in Table 1.

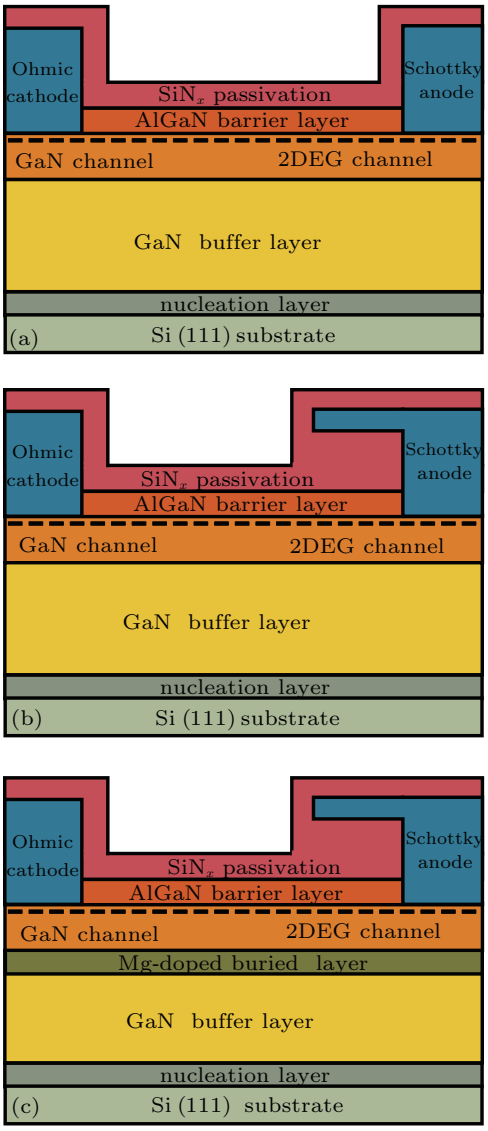


Fig. 1. (color online) Cross-sectional views of the proposed device structures of (a) conventional AlGaN/GaN Schottky barrier diode, (b) anode-connected-field-plate AlGaN/GaN Schottky barrier diode, and (c) anode-connected-field-plate AlGaN/GaN Schottky barrier diode with magnesium-doped p-type buried layer.

Table 1. Material parameters for simulation.

Parameters	AlGaN	GaN
Bandgap/eV	3.82	3.4
Electron mobility/cm^{-2}·V^{-1}·s^{-1}	550	1100
Electron saturation velocity/cm·s^{-1}	2×10^7	2×10^7
Dielectric constant	9.5	9.5

3. Electric field modulation of AFP

Lateral power devices generally employ the field plate technologies for the drift region design, in order to achieve a low on-resistance and a high breakdown voltage at the same time.[14] In the simulation, we first evaluate the V_B performance of AlGaN/GaN Schottky barrier diode with anode-connected-field-plate only (AFP-SBD). In comparison with the conventional AlGaN/GaN SBD, a wide electron depletion length in the drift region is achieved due to the extended potential line by the AFP (see Figs. 2(a) and 2(b)). The electric field modulation by the AFP brings an electric strength elevation in the 2DEG channel with a laterally distributed direction A, thus increasing the V_B significantly (see Figs. 2(c) and 2(d)).

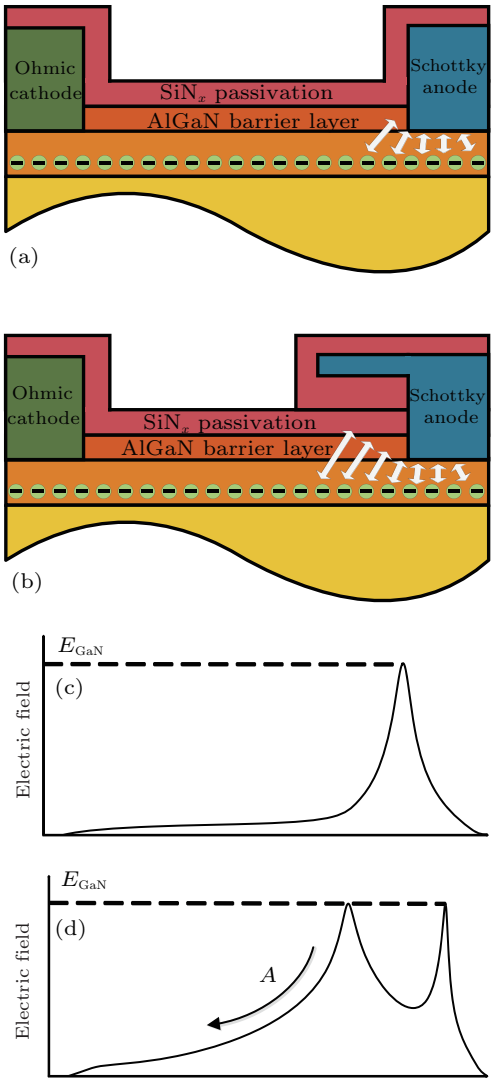


Fig. 2. (color online) Schematic views of depletion method and breakdown electric field of conventional AlGaN/GaN SBD [panels (a) and (c)] and AlGaN/GaN SBD with anode-connected field plate [panels (b) and (d)].

Figure 3(a) shows plots of the simulated V_B as a function of AFP geometry variables including T_{AFP} and L_{AFP}. Results show that novel AFP-SBD with a total drift region length of 10.5 μm can achieve V_B as high as 1.2 kV with an optimized AFP of $T_{AFP} = 0.5$ μm and $L_{AFP} = 2.0$ μm, while Con. SBD with the same physical dimensions suffers from the electric field crowding around the Schottky junction region and bears

only a poor V_B of 280 V. However, independent of the AFP geometry, the high fields are always restricted into a region with a certain width below the AFP and electrodes, leaving most of the drift region with comparatively very low fields, thus revealing incomplete electron depletion in the drift region (see Fig. 3(b)). As a result, it is still a problem in further increasing the V_B for AFP-SBD, owing to the limitation of the AFP electric field modulation.

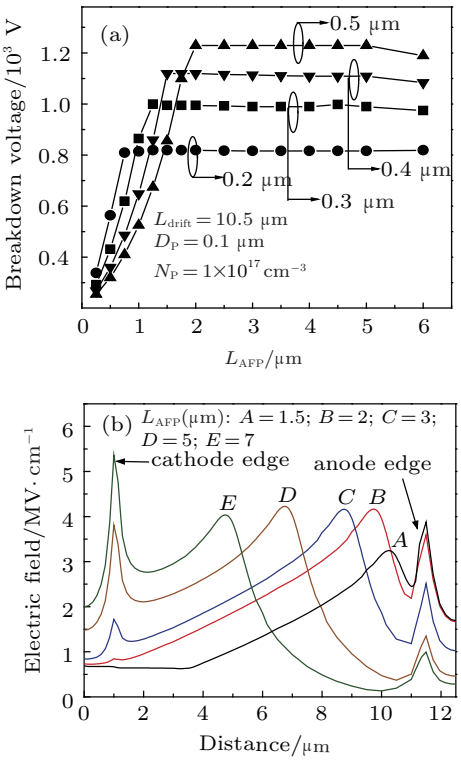


Fig. 3. (color online) (a) Plots of breakdown voltage as a function of L_{AFP} with different values of T_{AFP} for AlGaN/GaN Schottky barrier diode with anode-connected-field-plate only, (b) plots of breakdown channel field distribution of the AFP-SBD with various values of L_{AFP} at $T_{AFP} = 0.5$ μm. (The Selberherr impact ionization model parameters used in this paper are as follows: $an_1 = 2.9\times10^8$ cm^{-1}, $an_2 = 2.9\times10^8$ cm^{-1}, $bn_1 = 2.452\times10^7$ V/cm, $bn_2 = 2.452\times10^7$ V/cm, $ap_1 = 2.9\times10^8$ cm^{-1}, $ap_2 = 2.9\times10^8$ cm^{-1}, $bp_1 = 2.452\times10^7$ V/cm, $bp_2 = 2.452\times10^7$ V/cm).

4. Bulk electric field modulation of p-type buried layer

To further modulate the electric field in the drift region, a magnesium-doped p-type buried layer is employed to enhance the electron depletion at reverse bias as shown in Fig. 4(a). Figure 4(b) shows the breakdown electric field vertical cutlines of both AFP-SBD and AFP-RESURF-SBD at the cathode electrode end.

In AFP-SBD, the electron depletion is confined only in the region below the field plate, leaving the most part of the bulk layer in a rather incomplete depleted state. As a result, the electric field in the channel region is only modulated by the AFP geometry laterally and the incomplete depleted bulk region field is passively affected by the more intensive depleted surface channel field with the downward direction *B*, as shown in Fig. 4(b). In AFP-RESURF-SBD, as a comparison, the electrons are depleted by both field plate and bulk PN junction. With the enhanced electron depletion, the electric field in the bulk region is significantly elevated to a certain high level to modulate the surface channel field with the upward direction *C*. In this case, the channel electric field is modulated by the AFP electron depletion laterally and the PN junction depletion vertically. With the 2D modulation, the fully depleted channel and bulk region reveal much higher fields with uniformly distributed field profiles.

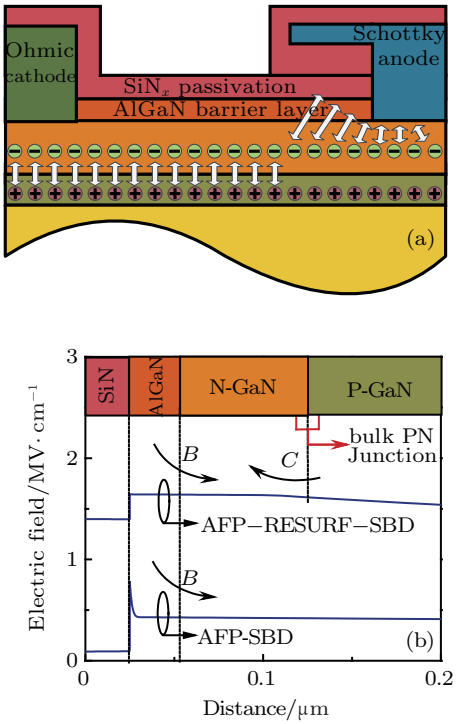


Fig. 4. (color online) (a) Schematic cross-sectional view of the depletion mode for the AlGaN/GaN SBD with anode-connected field plate and magnesium-doped p-type buried layer, (b) vertical cutlines of the electric field at the cathode end for AFP-SBD and AFP-RESURF-SBD at breakdown.

Figure 5 shows the electron concentration distributions and the electric field distributions at breakdown for AFP-SBD and AFP-RESURF-SBD. Both devices have an optimized AFP of $T_{AFP} = 0.5$ μm and $L_{AFP} = 2.0$ μm as mentioned in Section 3. In Figs. 5(a) and 5(b), more electrons are depleted in the AFP-RESURF-SBD than those in the AFP-SBD, both in the channel and in the bulk region. Especially in the region between AFP and the cathode electrode, the electron concentration is much lower in AFP-RESURF-SBD than that in AFP-SBD as shown in Fig. 5(c). With the more intensive depletion, the bulk field is raised to modulate the channel field to a much higher level with a third field peak introduced around the cathode end as shown in Fig. 5(d). So it is obvious that the implementation of the p-type buried layer in AFP-RESURF-SBD is effective in enhancing the electron depletion and breakdown strength through the additional bulk field modulation compared with the case in the AFP-SBD.

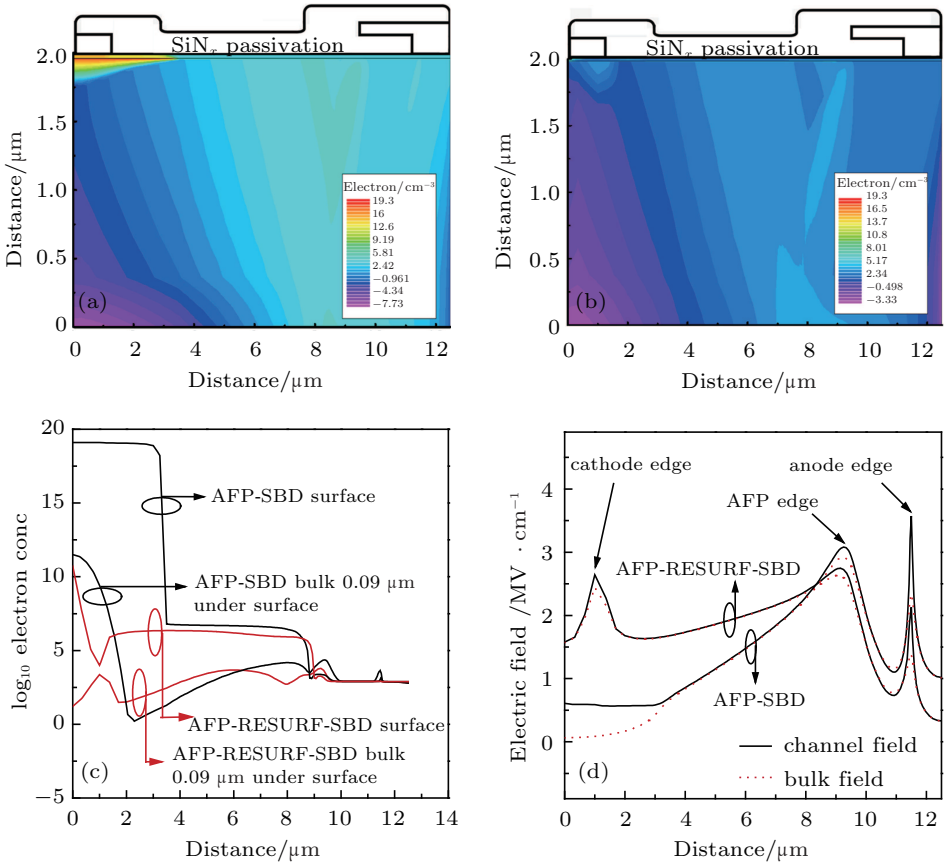


Fig. 5. (color online) Electron concentration distributions at breakdown of (a) AFP-AlGaN/GaN-SBD, (b) novel AlGaN/GaN AFP-RESURF-SBD with $T_P = 0.28$ μm, $N_P = 1 \times 10^{17}$ cm^{-3}, (c) lateral cutlines of electron distribution of both devices in channel region and bulk region at breakdown, (d) lateral cutlines of electric field distribution in channel region and bulk region of both devices at breakdown.

5. Optimization of the bulk electric field modulation

As the bulk electric field modulation of the AFP-RESURF-SBD is proved to be effective in enhancing the V_B of AlGaN/GaN SBDs, further optimization of the p-type buried layer parameters (p-type buried layer thickness, T_P and magnesium doping concentrations, N_P) is investigated.

The optimal bulk electric field modulation region dosage is determined by the Gauss law,

$$\int \xi \cdot \mathrm{d}A \approx \xi \cdot A = -Q/\varepsilon_s, \quad N_{opt} = Q_{opt}/qA \approx \xi\varepsilon_s/q,$$

where ξ is the critical field of the semiconductor, q is electron charge, Q_{opt} is the optimal bulk electric field modulation region space charge, and N_{opt} is optimal bulk electric field modulation dosage. For silicon, the optimum buried layer dose is around 10^{12} cm^{-2}. For an ideal GaN material, due to its critical field being 10 times larger than that of the silicon, the optimal buried layer dose is about 10^{13} cm^2. As mentioned in Section 4, the bulk field modulation principle is to introduce additional negative space charges, which are provided by the p-type buried layer, to balance the positive space charges, which are contained in the n-type 2DEG channel layer in the off-state. In our case of AFP-RESURF-SBD, the charge balance is realized through the collaboration of both AFP and p-type buried layer, which means that a part of the positive space charges are balanced through the AFP while the other part of the charges are balanced through the p-type buried layer. As a result, the magnesium dose of the p-type buried layer is expected to be less than 10^{13} cm^2. Through simulation, p-type buried layers with various values of thickness (T_P) and doping concentration (N_P) are analyzed in the optimized AFP-SBD structure acquired in Section 3. Figure 6(a) shows the bulk electric field optimization procedure on the V_B through a function of T_P with different values of N_P. All three values of doping concentration (N_P) can achieve a maximum V_B of about 1.8 kV with different values of p-type layer thickness (T_P) correspondingly, which shows a strong proof of charge balance effect of the bulk field modulation. However, curves of different values of N_P reveal very different changing rates. Considering further experimental studies of the AFP-RESURF-SBD, including the growth of GaN epitaxial wafer with uniformly p-type buried layers, a very moderate and controllable p-type layer profile of $N_P = 1 \times 10^{17}$ cm^{-3} is recommended, since the V_B is too sensitive to the T_P in curve with $N_P = 5 \times 10^{16}$ cm^{-3} and $N_P = 5 \times 10^{17}$ cm^{-3} is technically hard to achieve under normal wafer manufacturing conditions.

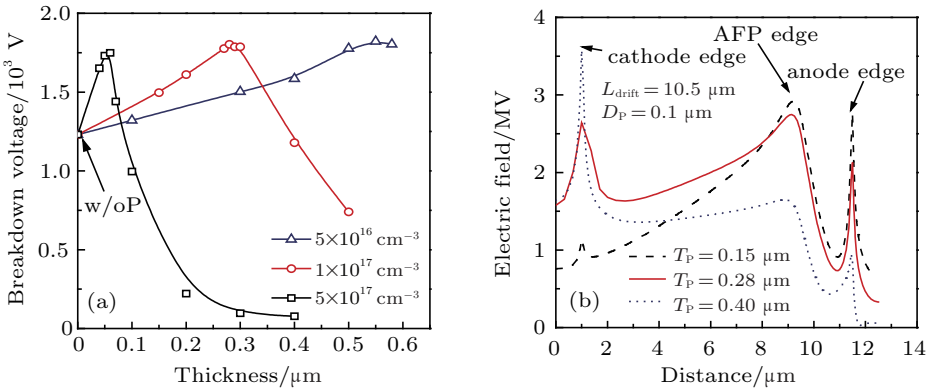


Fig. 6. (color online) (a) Plots of breakdown voltage versus p-type layer thickness with different p-type doping concentrations, and (b) channel electric field distributions of devices with different values of p-type layer thickness at $N_P = 1 \times 10^{17}$ cm^{-3}.

For the magnesium doping concentration of 1×10^{17} cm^{-3}, $V_{B\,max} = 1803$ V is obtained at a thickness of 0.28 μm. One thing that needs to be stressed in Fig. 6(b) is that the accurate magnesium dosage for charge balance is crucial in order to realize an ideal bulk field modulation with equally strengthened electric field peaks both under electrodes and on the AFP edge in the channel. The reshaped channel field distribution shows good agreement with previous results presented by other groups.[15] On the contrary, charge unbalance conditions are also discussed. For example, when the magnesium p-type buried layer thickness is less than 0.28 μm, the p-type buried layer cannot provide enough charges to balance the charges provided by the 2DEG channel layer and the weakened bulk field through PN depletion cannot effectively modulate the channel field which, as a result, leads to an AFP-field-modulation-dominated electric field. For a specific case with $T_P = 0.15$ μm, the V_B is lowered to 1.5 kV and the breakdown channel field distribution resembles strongly that of an AFP-SBD [see dashed line]. Meanwhile, when magnesium p-type layer thickness is larger than 0.28 μm, the charges provided by the p-type buried layer overwhelm those produced by the 2DEG channel layer. As a result, the enhanced vertical PN depletion will lead a PN-bulk-field-modulation dominated electric field, producing a high field peak below the cathode. For a specific case with $T_P = 0.40$ μm [see dotted line], the V_B is lowered to 1.2 kV, which shows a deterioration and is even worse than the structure with $T_P = 0.15$ μm.

It is important to notice that although a significant improvement on the value of V_B is achieved through the field-modulation techniques, possible deterioration of the current transport in the forward characteristics could be predicted. Due to the elevated conduction band of the p-type buried layer in the bulk region, the 2DEG channel is confined and electrons along the channel region are partially depleted, thus making the current conduction decrease and R_{on} increase inevitably. However, as AlGaN/GaN devices take advantage of the unique 2DEG as a current path, it is the electrons (commonly with a concentration of 10^{19}/cm^3) in the quantum well which is located exactly at the GaN-side heterojunction interface that take part most in the current transport. On the contrary, electrons distributed far deep in the bulk region with comparatively low concentrations (commonly 4–6 orders of magnitude lower) barely take part in the current transport and can lead to vertical leakage current through the dislocation densities of the GaN buffer.[16] Numerical analysis shows that with proper location (D_p), the reduction of the effect of the current conduction and the increase of R_{on} can be minimized. Figures 7(a) and 7(b) show the conduction band energy and 2DEG electron concentration distributions of the AFP-SBD and APF-RESURF-SBDs. All three APF-RESURF-SBDs are with the optimized p-type buried layer parameters (T_P/N_P) extracted from Fig. 5(a), and have 5×10^{16} cm^{-3}/0.58 μm, 1×10^{17} cm^{-3}/0.28 μm, and 5×10^{17} cm^{-3}/0.05 μm, respectively. With a properly designed p-type layer depth of 0.1 μm, the quantum well structure and 2DEG distributions with minor deterioration are achieved. Detailed structures show that these specific channel regions are safe from the p-type layer depletion effect. Figure 7(c) shows the forward characteristics of the AFP-SBD and APF-RESURF-SBDs. With the minor reduction of the current transport ability, all three optimized structures each reveal an improvement on yielding the GaN limit at the expense of losing 10%, 17%, and 25% conduction ability, which is traded for the 50% enhancement of the value of V_B. The calculations of the power device figure-of-merit (FOM) $BV^2/R_{on\cdot sp}$ also show 111%, 92%, and 78% improvement for these three devices respectively.

Finally, a profile of the electric field optimization for an AFP-RESURF-SBD is shown in Fig. 8. Within the inverse-function-like curve, a randomly selected point (see open square) also guarantees a high V_B of 1.8 kV in the simulation. This profile offers strong support for the charge balance theory of the bulk field modulation effect and an empirical guideline in further experimental studies of the AFP-RESURF-SBD fabrications that are now in process.

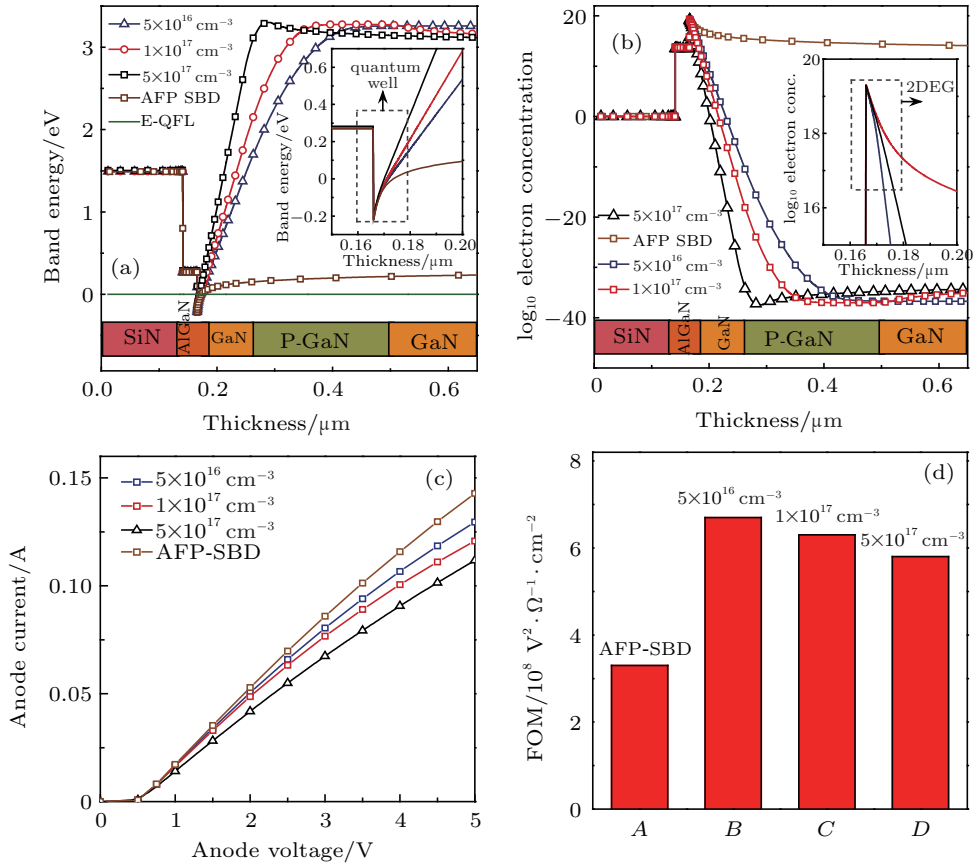


Fig. 7. (color online) (a) Vertical cutlines of conduction band energy of the AFP-SBD and optimized AFP-RESURF-SBD, (b) vertical cutlines of electron concentration of the AFP-SBD and optimized AFP-RESURF-SBD, (c) forward characteristics of the AFP-SBD and optimized AFP-RESURF-SBD, (d) power device FOMs of the AFP-SBD and optimized AFP-RESURF-SBD.

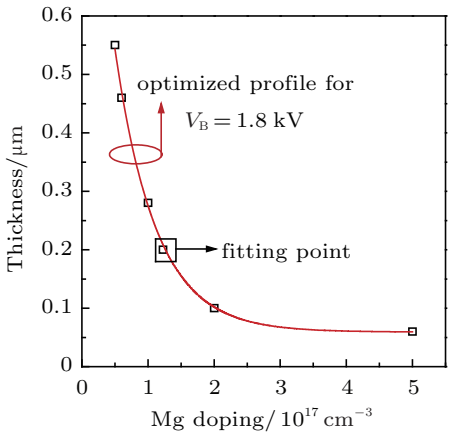


Fig. 8. (color online) Optimized thickness of AFP-RESURF-SBD as a function of magnesium layer concentration and thickness.

6. Conclusions

In this paper we comprehensively investigate the effect of the bulk electric field modulation of the magnesium p-type buried layer on the value of V_B for an AlGaN/GaN FP-RESURF-SBD. Using 2D simulations, a systematic procedure is proposed for modulating the electric field and the parameters of optimized AlGaN/GaN FP-RESURF-SBD are calculated. The value of V_B can be increased 5 times using AFP with $T_{AFP} = 0.5$ μm, $L_{AFP} = 2.0$ μm, and magnesium p-type buried layer $T_P = 0.28$ μm, $N_P = 1 \times 10^{17}$ cm^{-3}, yielding a theoretical limit of GaN-based material.

References

[1] Pengelly R S, Wood S M, Milligan J W, Sheppard S T and Pribble W L 2012 *IEEE Trans. Microwave Theory and Techniques* **60** 1764

[2] Selvaraj S, Suzue T and Egawa T 2009 *IEEE Electron Dev. Lett.* **30** 587

[3] Wang H, Liang H, Wang Y, Ng K W, Deng D M and Lau K M 2010 *Chin. Phys. Lett* **27** 038103

[4] Xie G, Xu E, Niloufar H, Zhang B, Fu Y F and Ng W T 2012 *Chin. Phys. B* **21** 086105

[5] Guo L L, Feng Q, Ma X B, Hao Y and Liu J 2007 *Acta Phys. Sin.* **56** 2900 (in Chinese)

[6] Lee S C, Ha M W, Her J C, Kim S S, Lim J Y, Seo K S and Han M K 2005 *ISPSD*, May 23–26, Santa Barbara, USA, p. 247

[7] Wang M J and Chen J K 2011 *IEEE Trans. Electron Dev.* **58** 460

[8] Narita T, Kikuta D, Iguchi H, Ito K, Tomita K, Uesugi T and Kachi T 2012 *Phys. Status Solidi C* **9** 915

[9] Duan B X and Yang Y T 2012 *Chin. Phys. B* **21** 057201

[10] Treidel E B, Hilt O, Zhytnytska R, Wentzel A, Meliani C, Wuerfl J and Traenkel G 2012 *IEEE Electron Dev. Lett.* **33** 357

[11] Quay R 2008 *Gallium Nitride Electronics* (Berlin: Springer-Verlag)

[12] Wei W, Lin R B, Feng Q and Hao Y 2008 *Acta Phys. Sin.* **57** 467 (in Chinese)

[13] Kunihiro K, Kasahara K, Takahashi Y and Ohno Y 1999 *IEEE Electron Dev. Lett.* **20** 608

[14] Karmalkar S and Mishra U K 2001 *IEEE Electron Dev. Lett.* **48** 1515

[15] Nakajima A, Shimizu M and Okumura H 2007 *Phys. Status Solidi C* **4** 2736

[16] Zhang J C, Dong Z D, Qin X X, Zheng P T, Liu L J and Hao Y 2009 *Acta Phys. Sin.* **58** 1959 (in Chinese)